

This discussion paper is/has been under review for the journal *Atmospheric Chemistry and Physics (ACP)*. Please refer to the corresponding final paper in *ACP* if available.

**NO₂ DOAS
measurements at
Tenango del Aire**

M. L. Melamed et al.

Detection of pollution transport events southeast of Mexico City using ground-based visible spectroscopy measurements of nitrogen dioxide

M. L. Melamed¹, R. Basaldud¹, R. Steinbrecher², S. Emeis², L. G. Ruíz-Suárez¹, and M. Grutter^{1,*}

¹Centro de Ciencias de la Atmósfera, Univ. Nacional Autónoma de México, México D.F., México

²Institute for Meteorology and Climate Research, Atmospheric Environmental Research (IMK-IFU), Forschungszentrum Karlsruhe GmbH, Garmisch-Partenkirchen, Germany

* now at: Institut für Meteorologie und Klimaforschung, Karlsruhe, Germany

Received: 19 December 2008 – Accepted: 12 January 2009 – Published: 24 February 2009

Correspondence to: M. L. Melamed (megan.melamed@gmail.com)

Published by Copernicus Publications on behalf of the European Geosciences Union.

Title Page

Abstract

Introduction

Conclusions

References

Tables

Figures

◀

▶

◀

▶

Back

Close

Full Screen / Esc

Printer-friendly Version

Interactive Discussion



Abstract

This work presents ground based differential optical absorption spectroscopy (DOAS) measurements of nitrogen dioxide (NO_2) during the MILAGRO field campaign in March 2006 at the Tenango del Aire research site located to the southeast of Mexico City. The DOAS NO_2 column density measurements are used in conjunction with ceilometer, meteorological and surface nitrogen oxides (NO_x) and total reactive nitrogen (NO_y) measurements to show a more comprehensive view of air pollution results when a research site has both surface and remote sensing instruments. An in depth analysis of 13 March 2006 demonstrates how DOAS NO_2 , surface NO_2 and ceilometer data can be used to determine the extent of mixing of the pollution layer. In addition, we show the effectiveness of how DOAS measurements can be used to observe pollution sources that may reside above the mixing layer, such as the presence of lightning produced NO_2 as seen on 28 March 2006.

1 Introduction

Megacities (cities with a population greater than 10 million) play a critical role in local, regional and global air pollution. One megacity of primary interest is Mexico City, the world's second largest city with an estimated population of 22 million within an area of 7500 km^2 . Mexico City is located in the sub-tropics at 19° N and 99° W at 2240 m a.s.l. in a flat basin surrounded by mountains on three sides. The primary sources of pollution in Mexico City are transportation, industrial processes and domestic related activities. The high-density population, the unique geographical setting and multiple emission sources lead to high pollution episodes on a regular basis in Mexico City. These episodes have serious immediate and longer-term impacts on human health and the environment.

Recent research has begun to unravel the complexity of the air pollution problem in Mexico City and its effects not only on a local but on a regional and global scales

NO_2 DOAS measurements at Tenango del Aire

M. L. Melamed et al.

Title Page

Abstract

Introduction

Conclusions

References

Tables

Figures



Back

Close

Full Screen / Esc

Printer-friendly Version

Interactive Discussion



as well. Since 1986, an automated network for atmospheric monitoring in Mexico City (Red Automatica de Monitoreo Ambiental or RAMA) has been measuring surface mixing ratios of ozone (O_3), nitrogen oxides (NO_x), carbon monoxide (CO), sulfur dioxide (SO_2) and particulate matter (PM_{10}) (<http://www.sma.df.gob.mx/simat>). Meteorological data has been available since 1948 from the National Meteorology Service (<http://smn2.cna.gob.mx>). In addition to these continuous measurements, several large-scale, intensive field campaigns have augmented the data-base of air pollution and meteorological profiles. These include the Mexico City Air Quality Initiative (MARI 1990–1993), the Investigación sobre Materia Particulada y Deterioro Atmosferico-Aerosol and Visibility Research (IMADA-AVER 1997) and the Mexico City Metropolitan Area (MCMA 2003) experiment (Molina and Molina, 2002). In response to previous studies the Megacity Initiative: Local and Global Research Observations (MILAGRO 2006) campaign took place during March of 2006. The goal of MILAGRO 2006 was to use a team of international researchers to conduct measurements of gas phase and aerosol air pollutants in the Mexico City metropolitan area in order to study the transport and transformation of the measured air pollutants on local, regional and global scales (<http://www.eol.ucar.edu/projects/milagro/>).

The MILAGRO 2006 campaign had three primary surface research sites (T0, T1 and T2) to study the transport of pollution from the city center to the northeast. To date, many articles have been published from these three surface research sites (Doran et al., 2007; DeCarlo et al., 2008; Moffet et al., 2008; Querol et al., 2008; Stone et al., 2008; Thornhill et al., 2008; Hennigan et al., 2008, and references therein). Another research site located to the southeast of the city representing a background site was Tenango del Aire located at $19^{\circ}09'18''$ N and $98^{\circ}51'50''$ W at 2377 m. Figure 1 shows the location of the T0, T1, T2 and Tenango del Aire research sites. Tenango del Aire research site provides important information for the MILAGRO campaign since no other research sites were located to the south of the city even though winds blew from the city center to the south on many days throughout the campaign (de Foy et al., 2008). Here, we present an analysis of surface differential optical absorption spectroscopy

**NO₂ DOAS
measurements at
Tenango del Aire**M. L. Melamed et al.

[Title Page](#)[Abstract](#)[Introduction](#)[Conclusions](#)[References](#)[Tables](#)[Figures](#)[⏪](#)[⏩](#)[◀](#)[▶](#)[Back](#)[Close](#)[Full Screen / Esc](#)[Printer-friendly Version](#)[Interactive Discussion](#)

(DOAS) nitrogen dioxide (NO₂) column density measurements and show a more comprehensive analysis of urban air pollution results when a measurement site has both surface and remote sensing instruments.

2 Instrumentation and data analysis

- 5 The Tenango del Aire research site included DOAS measurements of NO₂, a ceilometer to determine the mixing layer height (MLH), surface measurements of nitrous oxide (NO), nitrogen oxides (NO_x), reactive nitrogen (NO_y) and surface meteorological data (temperature, humidity, wind direction and wind speed).

2.1 DOAS instrumentation and method

10 Scattered sunlight in the zenith view direction was collected with a small-sized telescope connected to a 600 μm diameter optical fiber. The optical fiber feeds the collected zenith sky sunlight to an Ocean Optics S2000 Miniature Fiber Optic Spectrometer with a TR-2 Thermoelectric Temperature Regulator. The S2000 is a commercially purchased crossed Czerny-Turner fixed grating spectrometer with a one-dimensional
15 (2048 pixel) charged coupled device (CCD) array, a 1200 line mm⁻¹ grating and a 50 μm entrance slit width resulting in an optical resolution of 1.07 nm full-width-half-maximum (FWHM) over the wavelength range from 418 to 731 nm. The integration time for zenith sky spectra was optimized to get a maximum signal under all conditions.

The visible zenith sky spectra are analyzed using the differential optical absorption spectroscopy (DOAS) method that has been extensively discussed by Platt (1994), Sanders (1996), Marquard et al. (2000). The DOAS method uses a Beer-Lambert type of equation to describe the attenuation of radiation by molecular absorbers between a foreground and background spectrum,

$$\frac{I_{FG}(\lambda)}{I_{BG}(\lambda)} = P(\lambda) \exp \left(- \sum_{i=0}^m S'_m \sigma'_m(\lambda) \right), \quad (1)$$

Title Page

Abstract

Introduction

Conclusions

References

Tables

Figures

◀

▶

◀

▶

Back

Close

Full Screen / Esc

Printer-friendly Version

Interactive Discussion



**NO₂ DOAS
measurements at
Tenango del Aire**

M. L. Melamed et al.

[Title Page](#)[Abstract](#)[Introduction](#)[Conclusions](#)[References](#)[Tables](#)[Figures](#)[◀](#)[▶](#)[◀](#)[▶](#)[Back](#)[Close](#)[Full Screen / Esc](#)[Printer-friendly Version](#)[Interactive Discussion](#)

where $I_{FG}(\lambda)$ is the foreground spectrum and $I_{BG}(\lambda)$ is the background spectrum. The background spectrum is a noon-time spectrum measured in clear skies and is characterized by the column densities of the absorbers in the non-polluted atmosphere. The foreground spectrum is a measured spectrum taken at a different time than the background spectrum. The polynomial, $P(\lambda)$, is used to describe the broad molecular absorption features and Rayleigh, aerosol and cloud scattering. The difference in molecular absorption between the foreground and background spectra is given by the sum of the differential molecular absorption cross sections of the species, $\sigma'_m(\lambda)$, times their differential slant column densities (DSCD), S'_m . To approximately account for the wavelength smoothing performed by the instrument, the molecular absorption cross sections are convolved by the slit function of the spectrometer used to measure the foreground and background spectra. It is important to note that since the background spectrum is taken from the ground and is not an extra-atmospheric spectrum of the sun, S'_m , is the difference in the slant column density of the absorber of interest between $I_{FG}(\lambda)$ and $I_{BG}(\lambda)$ and is not an absolute column measurement.

A critical step in the DOAS method is converting the DSCD to a vertical column density (VCD) by applying an appropriate air mass factor (AMF) that accounts for the increased optical path length through the atmosphere of the foreground spectrum relative to the vertical optical path length (Perliski and Solomon, 1993). To first approximation, the AMF of NO₂ column density measurements for solar zenith angles (SZA) less than $\sim 80^\circ$ is the secant of the SZA (Solomon et al., 1987). To determine the AMF for large SZA or for photons that are scattered multiple times due to the presence of clouds and aerosols often requires radiative transfer models. However, the retrieval of the oxygen collision complex (O₄) can provide important information in regards to the optical path length of the photons that have been scattered multiple times. The atmospheric O₄ mixing ratio is proportional to the square of the oxygen (O₂) mixing ratio and any non-pressure-related change in the absorption of visible light due to O₄ is an indicator of an increased optical path length due to multiple scattering in the atmosphere and not a true enhancement in the amount of O₄ in the atmosphere (Perner and

NO₂ DOAS measurements at Tenango del Aire

M. L. Melamed et al.

Title Page

Abstract

Introduction

Conclusions

References

Tables

Figures

◀

▶

◀

▶

Back

Close

Full Screen / Esc

Printer-friendly Version

Interactive Discussion



Platt, 1979; Greenblatt et al., 1990). It is important to note that since O₄ is an O₂–O₂ collision complex, the O₄ absorption cross section has the units cm⁵ molecules⁻². The O₄ “column densities” will be expressed with respect to the quadratic O₂ concentration in the units molecules² cm⁻⁵. Since these units are not traditional units for a molecular absorption cross section nor a column density, the O₄ quantities will use the symbol DSCD* throughout the text to denote this speciality.

In this study, the retrieved NO₂ DSCDs are converted to VCDs by applying an AMF of the secant of the SZA to account for the increase in absorption by NO₂ due to an enhanced optical path length through the stratospheric NO₂ layer at large SZA, Fig. 4. The resulting NO₂ VCD represents the enhancement in the NO₂ VCD due to pollution related events or increases in the optical path length due to multiple scattering by clouds and aerosols. The O₄ DSCD* are then used to give insight into the source and cause of the NO₂ VCD enhancements. This is done by calculating an AMF for O₄ according to Melamed et al. (2008), where the O₄ AMF, A_{O₄}, is defined as

$$A_{O_4} = \frac{S'_{O_4} + S_{BG,O_4}^*}{V_{O_4}^*}, \quad (2)$$

where S'_{O₄} is the retrieved O₄ DSCD*, S_{BG,O₄}^* is the calculated O₄ SCD* in the background spectrum and V_{O₄}^* is the calculated O₄ VCD* at the Tenango del Aire research site. If the vertical distribution of NO₂ and O₄ were identical then the O₄ AMF could be applied to the retrieved NO₂ DSCDs. However, since the vertical profiles of NO₂ and O₄ differ, the O₄ AMF is used in this study to qualitatively restrain the interpretation of the enhancements of the NO₂ VCDs.

NO₂ DSCDs are retrieved in the visible spectral window of 407–505 nm. In addition to NO₂, the other atmospheric absorbers included in the retrieval are O₃ and O₄. The high-resolution laboratory absorption cross section for O₃ at 223 K (Voigt et al., 2001), O₄ at 296 K (Greenblatt et al., 1990) and NO₂ at 293 K (Voigt et al., 2002) are convolved to the instrument resolution for use in Eq. (1). The analysis also includes a

**NO₂ DOAS
measurements at
Tenango del Aire**

M. L. Melamed et al.

Title Page

Abstract

Introduction

Conclusions

References

Tables

Figures

◀

▶

◀

▶

Back

Close

Full Screen / Esc

Printer-friendly Version

Interactive Discussion



Ring cross section derived according to Melamed et al. (2008) from the Kurucz et al. (1984) solar spectrum. A “shift and stretch” is applied to the foreground spectrum to align it in wavelength with the laboratory cross sections. The broad absorption and attenuation features are accounted for by including a second order polynomial.

5 The DOAS shift, stretch, polynomial coefficients and DSCDs are solved for using the Levenberg-Marquardt nonlinear least squares fitting algorithm (Lavenberg, 1944; Marquardt, 1963). The same background spectrum was used for the entire campaign and was taken on 18 March 2006 at 12:43 p.m. CDT when the SZA was the lowest for the entire day at 20°. This background spectrum was chosen because it was taken under
10 clear skies at a low SZA and when the surface NO₂ mixing ratio was small, 1.5 ppb. An example NO₂ DOAS retrieval is shown in Fig. 2. The estimated error in the NO₂ DOAS retrievals are $\pm 1.50 \times 10^{15}$ molecules cm⁻².

The O₄ DSCD*s are retrieved in a similar wavelength region as the NO₂ retrievals since photons in different wavelength regions can exhibit different optical path lengths, (Solomon et al., 1987; Platt et al., 1997). The O₄ DSCD*s are retrieved in the 460–
15 490 nm wavelength region. The O₄ retrievals include the following: a “shift and stretch”, a second order polynomial and the Ring, NO₂ and O₃ cross sections used in the NO₂ retrievals. The same background spectrum that was used in the NO₂ DOAS retrievals is used for the O₄ retrievals. An example O₄ DOAS retrieval is shown in Fig. 3. The
20 estimated error in the O₄ DOAS retrievals is $\pm 1.06 \times 10^{42}$ molecules² cm⁻⁵.

2.2 Ceilometer instrument and analysis

The ceilometer is a Vaisala double-lens ceilometer (Münkel et al., 2004). It measures the optical attenuated backscatter intensity at 0.855 μm averaged over 15 s. This special wavelength has been chosen because the absorption by water vapor is much
25 lower here than at 0.910 μm; a wavelength for which laser diodes are easily available. 0.885 μm would have been ideal but no laser diodes were available for this wavelength. The typical vertical range of this instrument is 4000 m; the vertical resolution used here

is 7.5 m. Apart from the very strong backscatter from clouds (that is what the instrument had originally been designed for) and fog, weaker gradients in the backscatter intensity are mainly determined by the number and the size spectrum of aerosol particles floating in the air. Reliable analysis of the vertical profile of particle-induced backscatter can be made from heights above ~ 140 m. Below that height the overlap between the emitted beam and the field-of-view of the receiver is smaller than 30%. The overlap is zero for heights below 60 m. Any signal received from distances below 60 m is generated by multiple scattering and scattering of light at dust and dirt particles on the weather protection glass of the transmitter into the field-of-view of the receiver. A slight contamination of the glass thus results in a signal amplitude decrease for distances above 60 m, but a signal amplitude increase for distances below 60 m (Emeis et al., 2007).

The MLH is retrieved using a refined approach of the retrieval by Schäfer et al. (2004), which is described in detail by Emeis et al. (2007). This retrieval algorithm is based on an analysis of the minima of the vertical gradients of the aerosol backscatter intensity (i.e. the greatest decreases in the backscatter intensity with height) recorded by the ceilometer.

Prior to the determination of gradient minima the overlap and range corrected attenuated backscatter profiles have to be averaged over time and height to suppress noise generated artefacts. Between 140 m and 500 m height sliding averaging is done over 15 min and a height interval Δh of 80 m. In the layer between 500 and 2000 m Δh for vertical averaging is extended to 160 m. Two additional parameters have been introduced to further reduce the number of false hits. The minimum accepted attenuated backscatter intensity right below a lifted inversion is set to $200 \times 10^{-9} \text{ m}^{-1} \text{ sr}^{-1}$ in the lower layer and $250 \times 10^{-9} \text{ m}^{-1} \text{ sr}^{-1}$ in the upper layer. Additionally the vertical gradient value of a lifted inversion must be more negative than $-0.30 \times 10^{-9} \text{ m}^{-1} \text{ sr}^{-1}$ in the lower layer and more negative than $-0.30 \times 10^{-9} \text{ m}^{-1} \text{ sr}^{-1}$ in the upper layer.

If $B(z)$ denotes the measured attenuated backscatter intensity in the height z above ground averaged over time and height and Δh is the height averaging interval, then

**NO₂ DOAS
measurements at
Tenango del Aire**M. L. Melamed et al.

[Title Page](#)[Abstract](#)[Introduction](#)[Conclusions](#)[References](#)[Tables](#)[Figures](#)[◀](#)[▶](#)[◀](#)[▶](#)[Back](#)[Close](#)[Full Screen / Esc](#)[Printer-friendly Version](#)[Interactive Discussion](#)

a gradient minimum is characterized by a change of sign from minus to plus of the second derivative of $B(z)$. The height interval under examination is searched from bottom to top for these gradient minima. There is a gradient minimum in the height z if the second derivative of $B(z)$ one range gate below z is not positive, if the second derivative of $B(z)$ in the height z is positive and if the false hit conditions mentioned above are fulfilled. The MLH from optical remote sensing is taken as the lowest height found by this procedure.

The retrieval algorithm for MLH fails in case of strong mist and fog and especially during rainfall because then the backscatter intensity is determined by the water or rain droplets only.

2.3 Surface mixing ratio measurements

NO_x , NO and NO_y surface concentrations were measured using a TEI 42C chemiluminescence monitor (Thermo Fisher Scientific Inc, 81 Wyman Street, Waltham, MA 02454) with several monitoring ranges spanning from 0–5 ppb and from 0–200 ppb with a linearity of $\pm 1\%$ of full scale reading. The lower detectable concentration is 50 ppt. When in NO_y mode, an additional Mo catalytic converter is used on top of the mobile unit and a short PFA Teflon inlet was used to minimize wall losses of nitric acid, HNO_3 (McClenny, 2000). All oxidized nitrogen species are converted to NO and measured as such in the TEI 42C instrument.

In the following analysis, the surface NO_2 mixing ratio is calculated from the NO_x and NO measurements ($[\text{NO}_2]=[\text{NO}_x]-[\text{NO}]$). On 21 March the NO_x and NO surface instrument switched to measuring NO_y and therefore the surface mixing ratio of NO_2 could not be determined after this date.

Title Page

Abstract

Introduction

Conclusions

References

Tables

Figures

◀

▶

◀

▶

Back

Close

Full Screen / Esc

Printer-friendly Version

Interactive Discussion



3 Results and discussion

The Tengango del Aire data set is divided into three case studies based on surface wind direction, surface NO_2 and NO_y concentrations and DOAS NO_2 VCD measurements as shown in Table 1. The three different cases are compared with the basin-scale wind analysis conducted by de Foy et al. (2008).

Case 1 days are dominated by northerly winds during the morning. Since the research site is located to the southeast of the city center, the surface mixing ratio and DOAS measurements detect various pollution plumes being transported through the research site when northerly winds exist. On the majority of the Case 1 days, the wind direction shifts mid- to late-afternoon from northerly to southerly. According to the basin-scale wind transport analysis conducted by de Foy et al. (2008), the Case 1 days are classified as South Venting (SV), O_3 -South (O_3S), or Cold Surge (CS) episodes. SV, O_3S and CS days were all dominated by northerly winds.

Case 2 days are all dominated by southerly winds. The surface mixing ratio and DOAS NO_2 measurements do not detect any significant increase in NO_2 throughout these days as the air to the south of the Tenango del Aire research site is relatively clean. The majority of Case 2 days are classified as O_3 -North (O_3N) episodes, which are dominated by southerly winds throughout the entire day (de Foy et al., 2008).

Case 3 days exhibit mainly southerly winds but the wind direction tends to be more variable throughout the day compared to the Case 1 and Case 2 days. In the mornings, the surface mixing ratio and DOAS NO_2 measurements do not detect any significant increase in air pollution. However, in the afternoon, the DOAS measurements indicate large enhancements in the NO_2 VCD while the surface NO , NO_x and NO_y mixing ratios show no corresponding increase. Case 3 days are classified as “convection-north” (CNVN) or “convection-south” (CNVS) episodes that are characterized by mostly clear skies in the morning, followed by afternoon showers and exhibited either a stronger north or south transport in the afternoon (de Foy et al., 2008).

In the following three sections, an “example” day from each case is analyzed in depth

Title Page

Abstract

Introduction

Conclusions

References

Tables

Figures

◀

▶

◀

▶

Back

Close

Full Screen / Esc

Printer-friendly Version

Interactive Discussion



and the importance of having both surface mixing ratio and remote sensing measurements at urban air pollution research sites in order to gain a more comprehensive understanding of air pollution is discussed. DOAS measurements are dependent on sufficient sunlight in order to make measurements. Therefore, the following days are analyzed from 07:45 to 17:45 local time (CDT) for $SZA < 80^\circ$.

3.1 Case 1 – 13 March 2006

A typical Case 1 day is 13 March 2006. On this day, northerly surface winds persisted at Tenango del Aire between 08:00 and 14:00 CDT. At 14:00, the wind direction shifts to southerly, Fig. 5. During the six hour period of northerly winds, the surface NO_2 measurements indicate three distinct plumes transported through the research site, Fig. 6. At 14:00 when the wind direction changes to southerly, the surface NO_2 mixing ratio decreases and the humidity increases as relatively clean air from the south is transported through the Tenango del Aire research site.

The first NO_2 Plume occurred early in the morning from 07:43 to 08:42 CDT and had a maximum surface NO_2 mixing ratio of 29 ppb. The mixing layer height (MLH) is low during this Plume with an average height of 312 ± 7 m. As can be seen in the NO_2 surface mixing ratio measurements, Plume 1 has two distinct peaks. The first peak occurs when the wind direction changed from southerly to northerly. The average wind speed during the first peak is less than 1 m s^{-1} . During the second peak of Plume 1, the wind direction is from the north, northeast and the wind speed increases from 0.2 m s^{-1} to 2.2 m s^{-1} . Due to the shift in the wind direction, it is likely that peak two of Plume 1 is actually the same air mass being transported through the research site for a second time due to the change in the wind direction. The width of the second peak should therefore be narrower than the width of the first peak since the wind speed was significantly higher during the second peak. Figure 6 indicates that the second peak is indeed narrower than the first peak. The DOAS NO_2 measurements do not detect the first plume. This suggests Plume 1 is a thin low lying NO_2 layer that cannot be detected by the DOAS measurements because the column density is small.

NO_2 DOAS measurements at Tenango del Aire

M. L. Melamed et al.

Title Page

Abstract

Introduction

Conclusions

References

Tables

Figures

◀

▶

◀

▶

Back

Close

Full Screen / Esc

Printer-friendly Version

Interactive Discussion



**NO₂ DOAS
measurements at
Tenango del Aire**

M. L. Melamed et al.

Title Page

Abstract

Introduction

Conclusions

References

Tables

Figures

◀

▶

◀

▶

Back

Close

Full Screen / Esc

Printer-friendly Version

Interactive Discussion



A second Plume from the north was transported through the Tenango del Air research site from 09:13 to 10:34 CDT. The average wind direction during Plume 2 was $12\pm 8^\circ$ and the average wind speed was $3.3\pm 0.8\text{ m s}^{-1}$. The maximum surface NO₂ mixing ratio was 30 ppb. The MLH begins to develop during Plume 2 increasing from 300 m to 500 m. Plume 2 is detected in the DOAS measurements due to an increase of NO₂ molecules in the atmosphere. As can be seen in Fig. 6, the NO₂ VCD reaches a maximum of 2.0×10^{16} molecules cm⁻².

A third NO₂ plume is transported through the Tenango del Aire research site from 10:45 to 11:58 CDT. The average wind direction during Plume 3 was still out of the north at $4\pm 18^\circ$ and the average wind speed was $3.8\pm 1.0\text{ m s}^{-1}$. During the passage of Plume 3, the MLH continued to increase to 1200 m and the maximum surface NO₂ mixing ratio was 32 ppb. Although the maximum surface NO₂ mixing ratio of Plume 3 is only slightly greater than the maximum surface NO₂ mixing ratio in Plume 2, the DOAS NO₂ VCD is much greater than the DOAS NO₂ VCD in Plume 2 with a maximum column density of 4.8×10^{16} molecules cm⁻². The column density measurements provide the total burden of the molecules in the atmosphere. Therefore the DOAS NO₂ VCD should increase between Plumes 2 and 3 as the number of NO₂ molecules in the atmosphere increases due to increased emissions from morning traffic. The surface NO₂ mixing ratio stayed more or less equal because the total number of the NO₂ molecules occupied more space due to the increase in MLH between Plumes 2 and 3. This highlights the difference between surface and column density measurement and the importance of having both measurement techniques at an urban research site.

After Plume 3, a smaller enhancement in the surface NO₂ mixing ratio and DOAS VCD measurements was observed. At 14:00 CDT when southerly winds dominated, both the surface mixing ratio and the column density of NO₂ decreased as relatively clean air was transported to the research site from the south. The winds were southerly for the rest of the day and no enhancements in the surface nor the DOAS NO₂ measurements were detected. The surface NO₂ mixing ratios indicate a background level NO₂ mixing ratio of 6.58 ± 0.79 ppb.

The O₄ AMF did not significantly increase during Plume 2 nor Plume 3 indicating the enhancements seen in the DOAS NO₂ VCD are due to an increase in pollution rather than an increased optical path length caused by multiple scattering by aerosols or clouds, Fig. 7. This conclusion is supported by the following comparison between the DOAS NO₂ VCDs and the surface NO₂ mixing ratio measurements.

Using the MLH from the ceilometer data, the DOAS NO₂ VCD can be used to estimate a mixing ratio assuming vertical homogeneity within the layer,

$$\text{NO}_2(\text{ppb}) = \frac{\text{NO}_2 \text{ VCD} * 1\text{e}9}{\bar{A}Z_B}, \quad (3)$$

where NO₂ VCD is the measured DOAS NO₂ VCD in molecules cm⁻², \bar{A} is the average number of air molecules in the ML in molecules cm⁻³ and Z_B is the MLH in m. If the ML is well mixed and the DOAS NO₂ VCD enhancement is located within the well mixed ML, then the calculated DOAS NO₂ mixing ratio should equal the surface NO₂ mixing ratio. Using Eq. (3), the DOAS NO₂ VCD are converted to a mixing ratio for Plumes 2 and 3. Figure 8 shows the measured surface and the calculated NO₂ mixing ratios agree well thus indicating that the ML is well mixed and the DOAS NO₂ VCD enhancement is due to an increase in pollution in the ML and not an increase in the optical path length of the photons.

3.2 Case 2 – 18 March 2006

18 March 2006 represents a Case 2 day, which were dominated by southerly winds and no significant enhancements in surface mixing ratio nor DOAS column densities of NO₂ were observed. On this day at the Tenango del Aire research site, the average wind direction was from the south at 191±25° from 07:45 to 17:45 CDT. The wind speed was rather constant with an average of 5.2±1.6 m s⁻¹, Fig. 9. As shown on the analysis of 13 March 2006, when the winds are from the south, the air passing through the Tenango del Aire research site is relatively clean. Figure 10 supports

[Title Page](#)
[Abstract](#)
[Introduction](#)
[Conclusions](#)
[References](#)
[Tables](#)
[Figures](#)
[Back](#)
[Close](#)
[Full Screen / Esc](#)
[Printer-friendly Version](#)
[Interactive Discussion](#)


this conclusion indicating the average surface NO₂ mixing ratio for the entire days was 2.88±1.93 ppb and never reached above 12 ppb. Between 07:45 and 09:45 CDT two small plumes can be identified in the surface NO₂ measurements. These low lying plumes are likely aged plumes either from Mexico City or from other urban areas to the south or southwest being transported through the Tenango del Aire research site as the wind direction shifted. In addition, throughout the day the surface measurements show narrow NO₂ enhancements. The source of the NO₂ in these peaks is most likely local and would not create any change in the DOAS NO₂ VCD. Therefore, the DOAS NO₂ VCD measurements show no enhancements throughout the entire day.

3.3 Case 3 – 28 March 2006

Case 3 days are classified by de Foy et al. (2008) as either CNVN or CNVS days, depending on the stronger component of transport in the late afternoon. These days occurred after humid conditions from a cold surge on 23 March 2006 persisted, leading to afternoon convection and rainfall (de Foy et al., 2008). Based on the meteorological data and the surface NO_y measurements, a Case 3 day appears to be very similar to a Case 2 day in that the dominate wind direction is from the south and no major enhancements were observed in the surface NO_y measurements. The large difference is that on all Case 3 days significant enhancements in the NO₂ DOAS VCD were observed in the afternoon that were not detected by the surface measurements.

An example Case 3 day is 28 March 2006, a CNVS day. On this day the average wind direction was from the southwest at 212±43° and the average wind speed was 3.2±1.3 m s⁻¹, Fig. 11. The surface NO_y mixing ratio measurements show no significant plumes throughout the day except for a low layer passing through the research site in the morning that coincides with the change in the wind direction in the morning from northerly to southerly, which was also observed on 13 and 18 March Fig. 12. Two enhancements in the DOAS NO₂ VCD were detected in the afternoon, a large one from 12:50 to 14:50 CDT followed by a smaller one from 13:00 to 16:20 CDT. Neither of these enhancements were detected in the surface NO_y mixing ratio measurements.

Title Page

Abstract

Introduction

Conclusions

References

Tables

Figures

◀

▶

◀

▶

Back

Close

Full Screen / Esc

Printer-friendly Version

Interactive Discussion



The following analysis will show that the NO₂ enhancements were likely due to a combination of an increased optical path length from multiple scattering within a cloud and an enhancement in NO₂ due to lightning produced NO.

Figure 13 shows the DOAS O₄ AMF for 28 March 2006. A large enhancement in the O₄ AMF and hence the optical photon path length was detected starting at 12:50 CDT and continuing until 14:50 CDT. In addition to an increased O₄ AMF, the intensity of the photons reaching the spectrometer decreases, indicating that the large enhancement in the optical path length is due to multiple scattering within thick clouds passing over the Tenango del Aire research site. The ceilometer data supports this conclusion detecting a cloud present above the Tenango del Aire research site from about 13:00 to 14:00 CDT and another cloud from 14:00 to 15:00 CDT, Fig. 14. The cloud height between 13:00 and 14:00 CDT was ~200 m a.g.l. and the height of the precipitating cloud between 14:00 and 15:00 CDT was ~500 m a.g.l. The algorithm for the retrieval of the the MLH fails during periods of rainfall, which are indicated by the pink circles in Fig. 14. Therefore, the MLH curve in Fig. 12 is not indicated past 12:30 CDT due to the presence of rain droplets.

The increase in the O₄ AMF during the first cloud was from 1.0 to 4.5 air masses. This increase in the O₄ AMF due to multiple scattering within the cloud accounts for the majority of the increase in the DOAS NO₂ VCD, but not all of it. A portion of the DOAS NO₂ VCD enhancement is therefore due to an actual increase in the column density of NO₂ due to lightning produced NO or an uptake of NO₂ into convective clouds from their surroundings, (Pickering et al., 1992; Solomon et al., 1999; Langford et al., 2004, and references therein). Lightning was detected in the vicinity of the Tenango del Aire research site on the afternoon of 28 March by the World Wide Lightning Location Network (WWLLN) suggesting that the NO₂ within the cloud could be due to lightning (<http://www.wwlln.net/>). However, doing an analysis to estimate the amount of NO₂ produced by lightning as done by Langford et al. (2004) or Fraser et al. (2007) is not possible due to the low resolution, ~20 km, of the WWLLN in Mexico and the lack of radar measurements.

**NO₂ DOAS
measurements at
Tenango del Aire**M. L. Melamed et al.

Title Page

Abstract

Introduction

Conclusions

References

Tables

Figures

◀

▶

◀

▶

Back

Close

Full Screen / Esc

Printer-friendly Version

Interactive Discussion



4 Conclusions

DOAS NO₂ VCD measurements were made during March 2006 as part of the MILA-GRO field campaign at the Tenango del Aire research site located to the southeast of Mexico City. Based on the DOAS NO₂ VCD measurements, in conjunction with surface meteorological and NO, NO_x and NO_y mixing ratio measurements, the data set was divided into three case studies. Case 1 days are characterized by northerly winds for the majority of the day, which transports several plumes from the north through the Tenango del Aire research site that are detected by both DOAS and surface NO₂ measurements. Case 2 days are characterized by southerly winds for the entire day. The air to the south is relatively clean and no major enhancements in the DOAS nor the surface NO₂ measurements are observed. Case 3 days appear to be very similar to Case 2 days in that the dominate wind direction was southerly and no major enhancements in the surface NO_y measurements were observed. However, during the afternoon on Case 3 days, the DOAS NO₂ measurements detect large NO₂ enhancements that are not observed in the surface NO_y measurements.

The combination of surface monitors and DOAS column density measurements, in conjunction with ceilometer and meteorological data, give the possibility to differentiate between localized and aged plumes, provide important information about the extent of mixing in the pollution layer and detected NO₂ enhancements above the MLH. The analysis of a Case 1 day, 13 March 2006, highlights the difference between DOAS column measurements and surface mixing ratio measurements. DOAS column density measurements observe the total burden of molecules in the atmosphere while surface mixing ratio measurements provide a localized concentration. Therefore, as shown in the analysis of 13 March 2006, surface mixing ratios across a variety of plumes can remain constant even though the DOAS column density measurements detect large changes in the total burden of NO₂ molecules in the atmosphere.

The DOAS column density measurements can also be used to estimate a mixing ratio if the MLH is well known. The measured surface mixing ratio should be equal to

NO₂ DOAS measurements at Tenango del Aire

M. L. Melamed et al.

Title Page

Abstract

Introduction

Conclusions

References

Tables

Figures

◀

▶

◀

▶

Back

Close

Full Screen / Esc

Printer-friendly Version

Interactive Discussion



the estimated DOAS mixing ratio if NO₂ is vertically homogeneous within the ML. This concept was tested using the DOAS NO₂ column density measurements on 13 March 2006. The analysis shows the NO₂ molecules in two plumes transported through the Tenango del Aire research site were well mixed.

5 The analysis of Case 3 days demonstrates the ability of DOAS measurements to determine the influence of pollution sources in the Mexico City basin that may reside above the ML. In addition to NO₂ produced from NO formed by lightning, other pollution sources that may reside above the ML are biomass burning and volcanic emission. Yokelson et al. (2007) suggests as much as 25% of NO_x emissions in the Mexico City
10 area during March 2006 were produced from mountain fires but much of these emissions could pass above surface monitors and not be detected. Raga et al. (1999) showed that sulfur dioxide emissions from the volcano Popocatepetl have a large influence on particulate sulfate matter in Mexico City but this influence is often not noticed until the following day when the volcanic SO₂ emissions have been mixed into the ML.
15 DOAS measurements of NO₂ and SO₂ could provide important information regarding these pollution sources.

Acknowledgements. This material is based upon work supported by the National Science Foundation International Research Fellowship Program under Grant No. 0653087, the SEMARNAT-CONACYT Grant No. C01-0116 and the MCMA 2006 project.

20 The authors acknowledge Ricard Torres Jardón and Alejandro Torres for the operation of the mobile laboratory at the Tenango del Aire research site.

References

de Foy, B., Fast, J. D., Paech, S. J., Phillips, D., Walters, J. T., Coulter, R. L., Martin, T. J., Pekour, M. S., Shaw, W. J., Kastendeuch, P. P., Marley, N. A., Retama, A., and Molina, L. T.: Basin-scale wind transport during the MILAGRO field campaign and comparison to
25 climatology using cluster analysis, *Atmos. Chem. Phys.*, 8, 1209–1224, 2008, <http://www.atmos-chem-phys.net/8/1209/2008/>. 4771, 4778, 4782, 4790

NO₂ DOAS measurements at Tenango del Aire

M. L. Melamed et al.

Title Page

Abstract

Introduction

Conclusions

References

Tables

Figures

◀

▶

◀

▶

Back

Close

Full Screen / Esc

Printer-friendly Version

Interactive Discussion



**NO₂ DOAS
measurements at
Tenango del Aire**

M. L. Melamed et al.

Title Page

Abstract

Introduction

Conclusions

References

Tables

Figures

◀

▶

◀

▶

Back

Close

Full Screen / Esc

Printer-friendly Version

Interactive Discussion

DeCarlo, P. F., Dunlea, E. J., Kimmel, J. R., Aiken, A. C., Sueper, D., Crounse, J., Wennberg, P. O., Emmons, L., Shinozuka, Y., Clarke, A., Zhou, J., Tomlinson, J., Collins, D. R., Knapp, D., Weinheimer, A. J., Montzka, D. D., Campos, T., and Jimenez, J. L.: Fast airborne aerosol size and chemistry measurements above Mexico City and Central Mexico during the MILAGRO campaign, *Atmos. Chem. Phys.*, 8, 4027–4048, 2008, <http://www.atmos-chem-phys.net/8/4027/2008/>. 4771

Doran, J. C., Barnard, J. C., Arnott, W. P., Cary, R., Coulter, R., Fast, J. D., Kassianov, E. I., Kleinman, L., Laulainen, N. S., Martin, T., Paredes-Miranda, G., Pekour, M. S., Shaw, W. J., Smith, D. F., Springston, S. R., and Yu, X.-Y.: The T1-T2 study: evolution of aerosol properties downwind of Mexico City, *Atmos. Chem. Phys.*, 7, 1585–1598, 2007, <http://www.atmos-chem-phys.net/7/1585/2007/>. 4771

Emeis, S., Jahn, C., Münkkel, C., Muensterer, C., and Schäfer, K.: Multiple atmospheric layering and mixing-layer height in the Inn valley observed by remote sensing, *Meteorologische Zeitschrift*, 16, 415–424, 2007. 4776

Fraser, A., Goutail, F., McLinden, C. A., Melo, S. M. L., and Strong, K.: Lightning-produced NO₂ observed by two ground-based UV-visible spectrometers at Vanscoy, Saskatchewan in August 2004, *Atmos. Chem. Phys.*, 7, 1683–1692, 2007, <http://www.atmos-chem-phys.net/7/1683/2007/>. 4783

Greenblatt, G. D., Orlando, J. J., Burkholder, J. B., and Ravishankara, A. R.: Absorption-Measurements of Oxygen between 330 nm and 1140 nm, *J. Geophys. Res.-Atmos.*, 95, 18 577–18 582, 1990. 4774

Hennigan, C. J., Sullivan, A. P., Fountoukis, C. I., Nenes, A., Hecobian, A., Vargas, O., Peltier, R. E., Case Hanks, A. T., Huey, L. G., Lefer, B. L., Russell, A. G., and Weber, R. J.: On the volatility and production mechanisms of newly formed nitrate and water soluble organic aerosol in Mexico City, *Atmos. Chem. Phys.*, 8, 3761–3768, 2008, <http://www.atmos-chem-phys.net/8/3761/2008/>. 4771

Kurucz, R., Furenchild, I., Brault, J., and Testermann, L.: Solar Flux from 296 nm to 1300 nm, *National Solar Observation Atlas*, Harvard Univertisty, Cambridge, Massachusetts, 240 pp., 1984. 4775

Langford, A. O., Portmann, R. W., Daniel, J. S., Miller, H. L., and Solomon, S.: Spectroscopic measurements of NO₂ in a Colorado thunderstorm: Determination of the mean production by cloud-to-ground lightning flashes, *Journal of Geophysical Research-Atmospheres*, 109, D11304, doi:10.1029/2003JD004158, 2004. 4783



- Lavenberg, K.: A Method for the Solution of Certain Problems in Least Squares, *Quart. Appl. Math.*, 2, 164–168, 1944. 4775
- Marquard, L. C., Wagner, T., and Platt, U.: Improved air mass factor concepts for scattered radiation differential optical absorption spectroscopy of atmospheric species, *J. Geophys. Res.-Atmos.*, 105, 1315–1327, 2000. 4772
- Marquardt, D.: An Algorithm for Least-Squares Estimation of Nonlinear Parameters, *SIAM J. Appl. Math.*, 11, 431–441, 1963. 4775
- McClenny, W.: Recommended Methods for Ambient Air Monitoring of NO, NO₂, NO_y and individual NO_z species, US Environmental Protection Agency, Triangle Park, NC 27711, Tech. rep., 2000. 4777
- Melamed, M. L., Langford, A. O., Daniel, J. S., Portmann, R. W., Miller, H. L., Eubank, C. S., Schofield, R., Holloway, J., and Solomon, S.: Sulfur dioxide emission flux measurements from point sources using airborne near ultraviolet spectroscopy during the New England Air Quality Study 2004, *J. Geophys. Res.-Atmos.*, 113, D02305, doi:10.1029/2007JD008923, 2008. 4774, 4775
- Moffet, R. C., de Foy, B., Molina, L. T., Molina, M. J., and Prather, K. A.: Measurement of ambient aerosols in northern Mexico City by single particle mass spectrometry, *Atmos. Chem. Phys.*, 8, 4499–4516, 2008, <http://www.atmos-chem-phys.net/8/4499/2008/>. 4771
- Molina, L. T. and Molina, M. J. (Eds.): *Air Quality in the Mexico Megacity: An Integrated Assessment*, vol. 2 of Alliance for Global Sustainability Bookseries, Kluwer Academic Publishers, Dordrecht, 384 pp., 2002. 4771
- Münkel, C., Emeis, S., Müller, W., and Schäfer, K.: Aerosol concentration measurements with a lidar ceilometer: results of a one year measuring campaign, vol. 5235 of *Remote Sensing of Clouds and the Atmosphere VIII*, Proc. SPIE, Bellingham, WA USA, 486–496, 2004. 4775
- Perliski, L. and Solomon, S.: On the Evaluation of Air Mass Factors for Atmospheric Near-Ultraviolet and Visible Absorption Spectroscopy, *J. Geophys. Res.-Atmos.*, 96, 10363–10374, 1993. 4773
- Perner, D. and Platt, U.: Detection of Nitrous-Acid in the Atmosphere by Differential Optical-Absorption, *Geophys. Res. Lett.*, 6, 917–920, 1979. 4773
- Pickering, K., Thompson, A., Scala, J., Tao, W., Dickerson, R., and Simpson, J.: Free Tropospheric Ozone Production Following Entrainment of Urban Plumes Into Deep Convection, *J. Geophys. Res.-Atmos.*, 97, 17,985–18,000, 1992. 4783

**NO₂ DOAS
measurements at
Tenango del Aire**M. L. Melamed et al.

[Title Page](#)[Abstract](#)[Introduction](#)[Conclusions](#)[References](#)[Tables](#)[Figures](#)[◀](#)[▶](#)[◀](#)[▶](#)[Back](#)[Close](#)[Full Screen / Esc](#)[Printer-friendly Version](#)[Interactive Discussion](#)

**NO₂ DOAS
measurements at
Tenango del Aire**

M. L. Melamed et al.

Title Page

Abstract

Introduction

Conclusions

References

Tables

Figures

◀

▶

◀

▶

Back

Close

Full Screen / Esc

Printer-friendly Version

Interactive Discussion



Platt, U.: Differential optical absorption spectroscopy (DOAS), in Air Monitoring by Spectroscopic Techniques, vol. 27-84 of Chemical Analysis: A series of monographs on analytical chemistry and its applications, John Wiley & Sons, INC., New York, sigris, m.w., 27–84, 1994. 4772

5 Platt, U., Marquard, L., Wagner, T., and Perner, D.: Corrections for zenith scattered light DOAS, Geophys. Res. Lett., 24, 1759–1762, 1997. 4775

Querol, X., Pey, J., Minguilln, M. C., Prez, N., Alastuey, A., Viana, M., Moreno, T., Bernab, R. M., Blanco, S., Crdenas, B., Vega, E., Sosa, G., Escalona, S., Ruiz, H., and Artano, B.: PM speciation and sources in Mexico during the MILAGRO-2006 Campaign, Atmos. Chem. Phys., 8, 111–128, 2008,
10 <http://www.atmos-chem-phys.net/8/111/2008/>. 4771

Raga, G. B., Kok, G. L., Baumgardner, D., Baez, A., and Rosas, I.: Evidence for volcanic influence on Mexico City aerosols, Geophys. Res. Lett., 26, 1149–1152, 1999. 4785

Sanders, R. W.: Improved analysis of atmospheric absorption spectra by including the temperature dependence of NO₂, J. Geophys. Res.-Atmos., 101, 20 945–20 952, 1996. 4772

15 Schäfer, K., Emeis, S., Rauch, C., Münkel, C., and Voigt, S.: Determination of mixing-layer heights from ceilometer data, vol. 5571 of Remote Sensing of Clouds and the Atmosphere IX, Proc. SPIE, Bellingham, WA USA, 248–259, 2004. 4776

Solomon, S., Schmeltekopf, A. L., and Sanders, R. W.: On the Interpretation of Zenith Sky Absorption-Measurements, J. Geophys. Res.-Atmos., 92, 8311–8319, 1987. 4773, 4775

20 Solomon, S., Portmann, R. W., Sanders, R. W., Daniel, J. S., Madsen, W., Bartram, B., and Dutton, E. G.: On the role of nitrogen dioxide in the absorption of solar radiation, J. Geophys. Res.-Atmos., 104, 12 047–12 058, 1999. 4783

Stone, E. A., Snyder, D. C., Sheesley, R. J., Sullivan, A. P., Weber, R. J., and Schauer, J. J.: Source apportionment of fine organic aerosol in Mexico City during the MILAGRO experiment 2006, Atmos. Chem. Phys., 8, 1249–1259, 2008,
25 <http://www.atmos-chem-phys.net/8/1249/2008/>. 4771

Thornhill, D. A., de Foy, B., Herndon, S. C., Onasch, T. B., Wood, E. C., Zavala, M., Molina, L. T., Gaffney, J. S., Marley, N. A., and Marr, L. C.: Spatial and temporal variability of particulate polycyclic aromatic hydrocarbons in Mexico City, Atmos. Chem. Phys., 8, 3093–3105, 2008,
30 <http://www.atmos-chem-phys.net/8/3093/2008/>. 4771

Voigt, S., Orphal, J., Bogumil, K., and Burrows, J. P.: The temperature dependence (203–293 K) of the absorption cross sections of O₃ in the 230–850 nm region measured by Fourier-

transform spectroscopy, J. Photochem. Photobiol. A, 143, 1–9, 2001. 4774

Voigt, S., Orphal, J., and Burrows, J. P.: The temperature and pressure dependence of the absorption cross-sections of NO₂ in the 250–800 nm region measured by Fourier-transform spectroscopy, J. Photochem. Photobiol. A, 149, 1–7, 2002. 4774

- 5 Yokelson, R. J., Urbanski, S. P., Atlas, E. L., Toohey, D. W., Alvarado, E. C., Crouse, J. D., Wennberg, P. O., Fisher, M. E., Wold, C. E., Campos, T. L., Adachi, K., Buseck, P. R., and Hao, W. M.: Emissions from forest fires near Mexico City, Atmos. Chem. Phys., 7, 5569–5584, 2007, <http://www.atmos-chem-phys.net/7/5569/2007/>. 4785

ACPD

9, 4769–4804, 2009

**NO₂ DOAS
measurements at
Tenango del Aire**

M. L. Melamed et al.

Title Page

Abstract

Introduction

Conclusions

References

Tables

Figures

⏪

⏩

◀

▶

Back

Close

Full Screen / Esc

Printer-friendly Version

Interactive Discussion



Table 1. Tenango del Aire days by case.

Date ¹	Case 1	Case 2	Case 3	SV	O ₃ S	O ₃ N	CS	CNVS	CNVN
2	X			X					
3	X			X					
4	X			X					
5	X			X					
6	X			X					
7	X			X					
8		X			X				
9		X				X			
10		X				X			
11		X				X			
12	X				X				
13	X			X					
14	X						X		
15	X				X				
16	X				X				
17	X				X				
18		X				X			
19		X				X			
20		X				X			
21	X						X		
22		X				X			
23	X						X		
24		X						X	
25		X						X	
26			X					X	
27		X							X
28			X						X
29			X						X
30			X						X
31			X					X	

¹ Day of month for March 2006 SV=South Venting, O₃S=O₃-South. O₃N=O₃-North, CS=Cold Surge, CNVS=Convection-South, CNVN=Convection-North (de Foy et al., 2008).

NO₂ DOAS measurements at Tenango del Aire

M. L. Melamed et al.

Title Page

Abstract

Introduction

Conclusions

References

Tables

Figures

◀

▶

◀

▶

Back

Close

Full Screen / Esc

Printer-friendly Version

Interactive Discussion





Fig. 1. Map of the Mexico City metropolitan area indicating the T0, T1 and T2 supersites as well as the Tenango del Aire research site to the southeast of the city center.

**NO₂ DOAS
measurements at
Tenango del Aire**

M. L. Melamed et al.

Title Page

Abstract

Introduction

Conclusions

References

Tables

Figures

◀

▶

◀

▶

Back

Close

Full Screen / Esc

Printer-friendly Version

Interactive Discussion



**NO₂ DOAS
measurements at
Tenango del Aire**

M. L. Melamed et al.

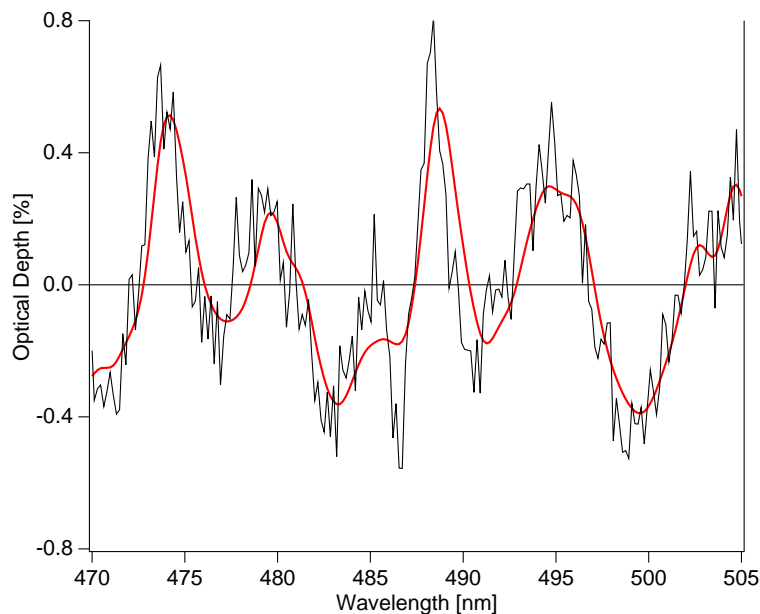


Fig. 2. The retrieved optical depth (red line) and the retrieved optical depth plus the residual of the nonlinear least squares fit (black line) of NO₂. The ~1% absorption corresponds to 5.5×10^{16} molecules cm⁻² measured on 13 March 2008 during Plume 2.

[Title Page](#)[Abstract](#)[Introduction](#)[Conclusions](#)[References](#)[Tables](#)[Figures](#)[◀](#)[▶](#)[◀](#)[▶](#)[Back](#)[Close](#)[Full Screen / Esc](#)[Printer-friendly Version](#)[Interactive Discussion](#)

**NO₂ DOAS
measurements at
Tenango del Aire**

M. L. Melamed et al.

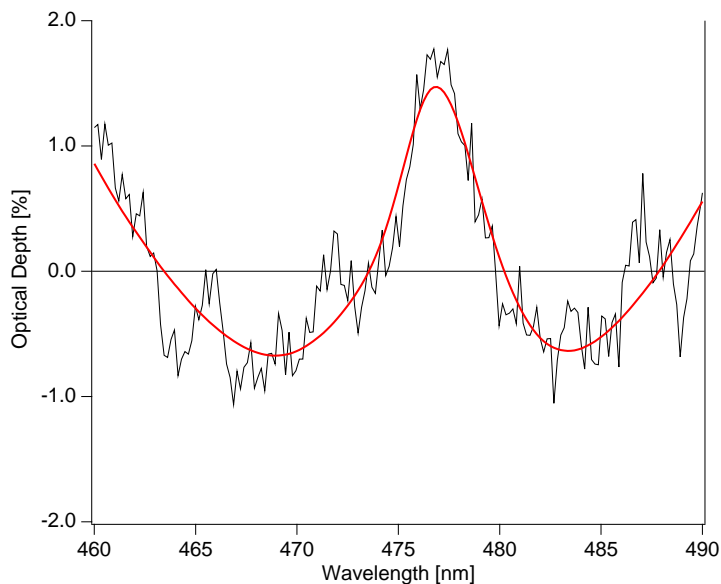


Fig. 3. The retrieved optical depth (red line) and the retrieved optical depth plus the residual of the nonlinear least squares fit (black line) of O₄. The ~2% absorption corresponds to 4.7×10^{43} molecules² cm⁻⁵ measured on 28 March 2008 during a thunderstorm. Please note O₄ is an O₂-O₂ collision complex and therefore the retrieved O₄ values are reported with respect to the quadratic of the O₂ concentrations in units molecules² cm⁻⁵.

[Title Page](#)[Abstract](#)[Introduction](#)[Conclusions](#)[References](#)[Tables](#)[Figures](#)[◀](#)[▶](#)[◀](#)[▶](#)[Back](#)[Close](#)[Full Screen / Esc](#)[Printer-friendly Version](#)[Interactive Discussion](#)

**NO₂ DOAS
measurements at
Tenango del Aire**

M. L. Melamed et al.

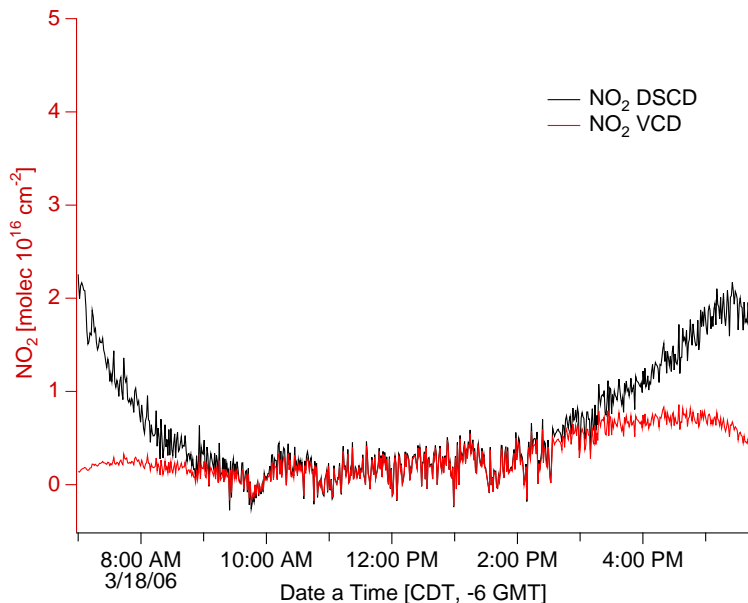


Fig. 4. The NO₂ DSCD (black line) is converted to the NO₂ VCD by applying an AMF of the sec(SZA) in order to account for the increased optical path length of photons as they travel through the stratospheric NO₂ layer at large SZA.

[Title Page](#)[Abstract](#)[Introduction](#)[Conclusions](#)[References](#)[Tables](#)[Figures](#)[◀](#)[▶](#)[◀](#)[▶](#)[Back](#)[Close](#)[Full Screen / Esc](#)[Printer-friendly Version](#)[Interactive Discussion](#)

**NO₂ DOAS
measurements at
Tenango del Aire**

M. L. Melamed et al.

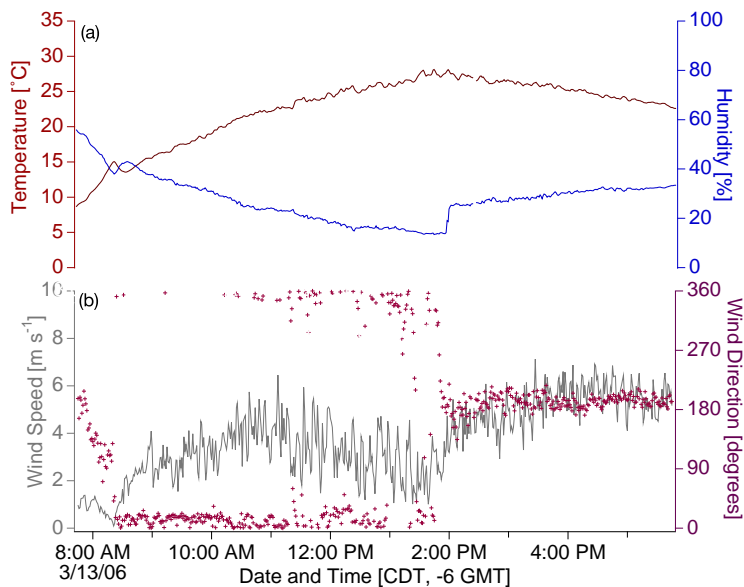


Fig. 5. Meteorological condition for 13 March 2006 at Tenango del Aire **(a)** air temperature and relative humidity and **(b)** wind speed and wind direction.

[Title Page](#)[Abstract](#)[Introduction](#)[Conclusions](#)[References](#)[Tables](#)[Figures](#)[◀](#)[▶](#)[◀](#)[▶](#)[Back](#)[Close](#)[Full Screen / Esc](#)[Printer-friendly Version](#)[Interactive Discussion](#)

**NO₂ DOAS
measurements at
Tenango del Aire**

M. L. Melamed et al.

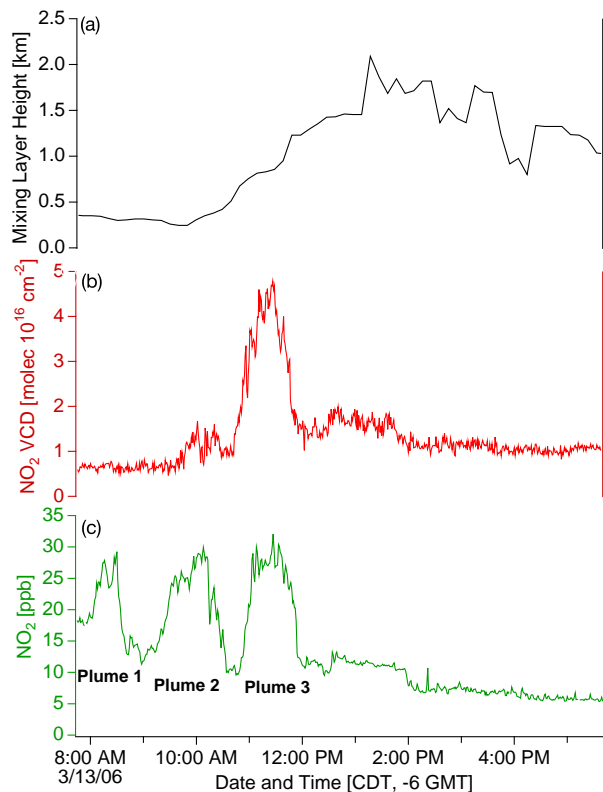


Fig. 6. Measurements of **(a)** ceilometer mixing layer height **(b)** DOAS NO₂ vertical column densities and **(c)** surface NO₂ on 13 March 2006. Plumes 1, 2 and 3 indicated three distinct NO₂ plumes that passed through the Tenango del Aire research site during the morning on 13 March 2006.

[Title Page](#)[Abstract](#)[Introduction](#)[Conclusions](#)[References](#)[Tables](#)[Figures](#)[◀](#)[▶](#)[◀](#)[▶](#)[Back](#)[Close](#)[Full Screen / Esc](#)[Printer-friendly Version](#)[Interactive Discussion](#)

**NO₂ DOAS
measurements at
Tenango del Aire**

M. L. Melamed et al.

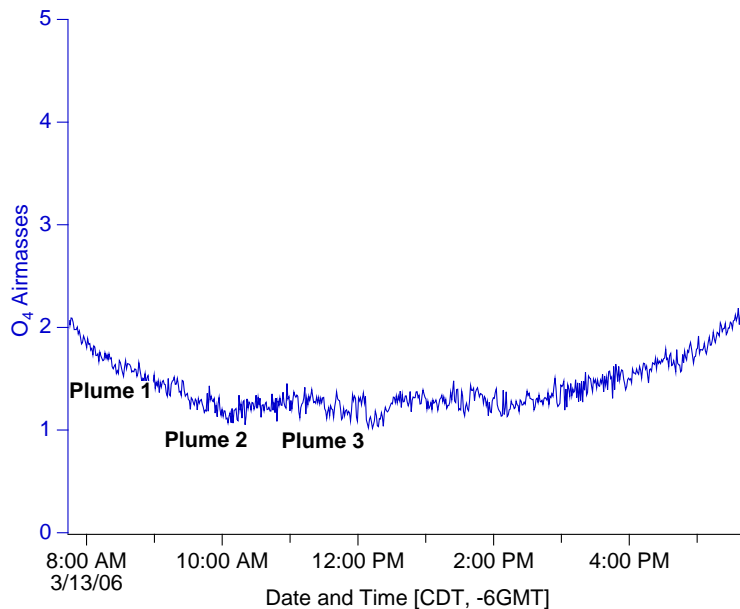


Fig. 7. The O₄ AMF for 13 March 2006. Plume 1, Plume 2 and Plume 3 represent the time period in which the NO₂ plumes passed through the Tenango del Aire research site on the morning of March 13th, 2006.

[Title Page](#)[Abstract](#)[Introduction](#)[Conclusions](#)[References](#)[Tables](#)[Figures](#)[◀](#)[▶](#)[◀](#)[▶](#)[Back](#)[Close](#)[Full Screen / Esc](#)[Printer-friendly Version](#)[Interactive Discussion](#)

**NO₂ DOAS
measurements at
Tenango del Aire**

M. L. Melamed et al.

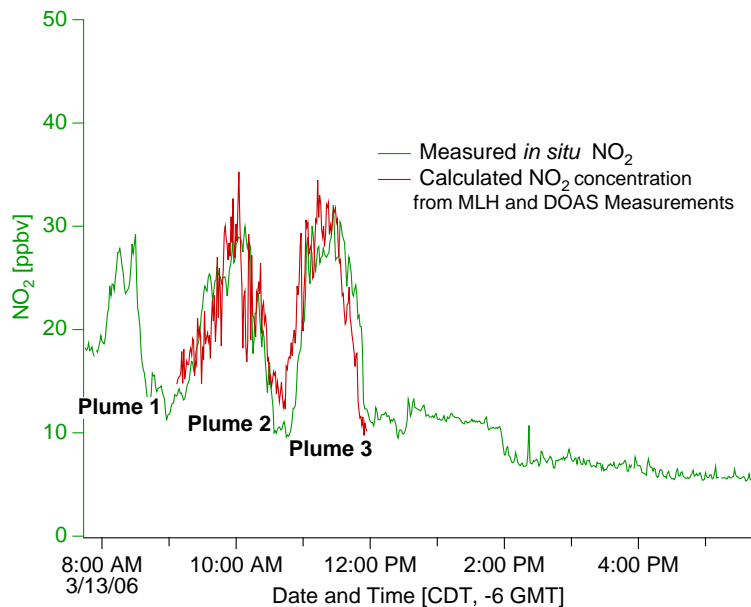


Fig. 8. A comparison of surface NO₂ measurements (green line) to calculated NO₂ mixing ratio in ppb from DOAS vertical column densities (red line) for Plume 2 and Plume 3 on 13 March 2006.

[Title Page](#)[Abstract](#)[Introduction](#)[Conclusions](#)[References](#)[Tables](#)[Figures](#)[◀](#)[▶](#)[◀](#)[▶](#)[Back](#)[Close](#)[Full Screen / Esc](#)[Printer-friendly Version](#)[Interactive Discussion](#)

**NO₂ DOAS
measurements at
Tenango del Aire**

M. L. Melamed et al.

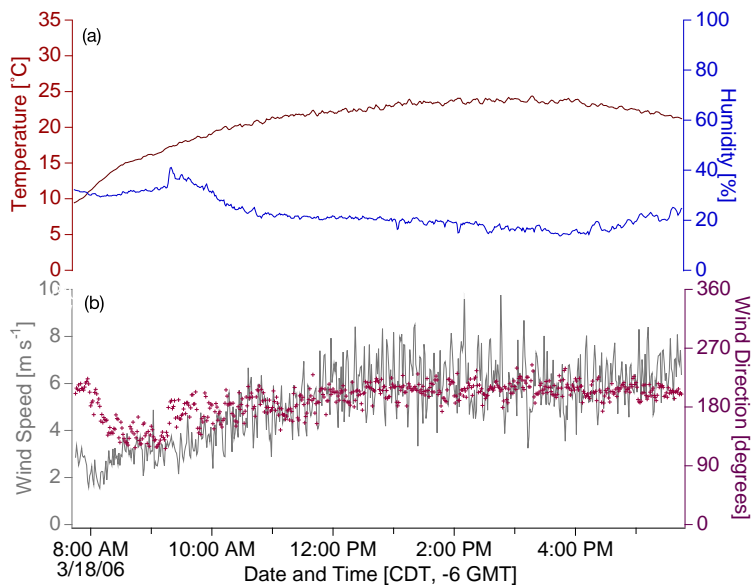


Fig. 9. Meteorological condition for 18 March 2006 at Tenango del Aire **(a)** air temperature and relative humidity and **(b)** wind speed and wind direction.

[Title Page](#)[Abstract](#)[Introduction](#)[Conclusions](#)[References](#)[Tables](#)[Figures](#)[◀](#)[▶](#)[◀](#)[▶](#)[Back](#)[Close](#)[Full Screen / Esc](#)[Printer-friendly Version](#)[Interactive Discussion](#)

**NO₂ DOAS
measurements at
Tenango del Aire**

M. L. Melamed et al.

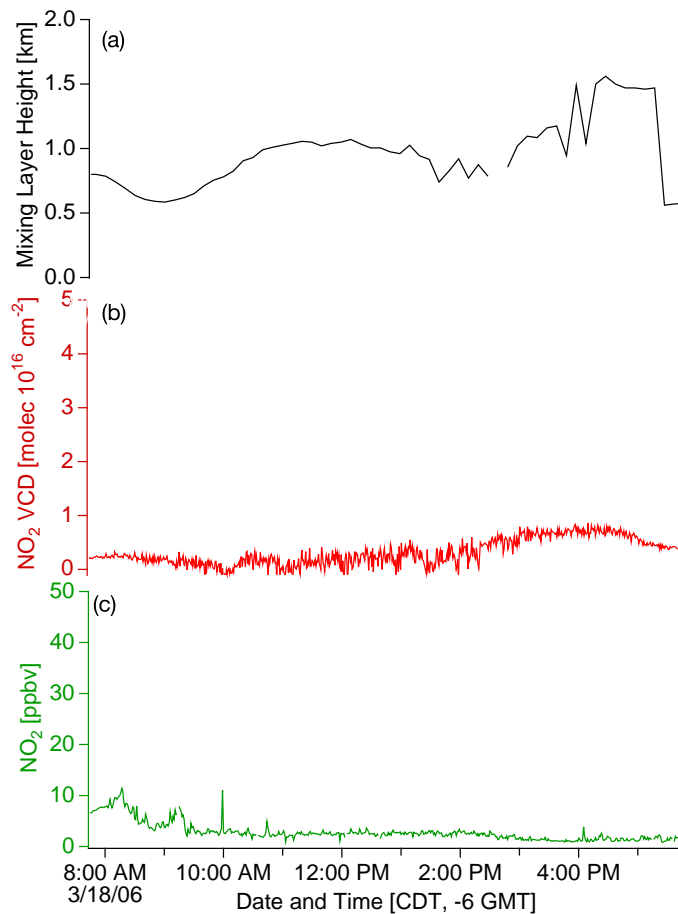


Fig. 10. Measurements of **(a)** ceilometer mixing layer height **(b)** DOAS NO₂ vertical column densities and **(c)** surface NO₂ on 18 March 2006.

[Title Page](#)[Abstract](#)[Introduction](#)[Conclusions](#)[References](#)[Tables](#)[Figures](#)[◀](#)[▶](#)[◀](#)[▶](#)[Back](#)[Close](#)[Full Screen / Esc](#)[Printer-friendly Version](#)[Interactive Discussion](#)

**NO₂ DOAS
measurements at
Tenango del Aire**

M. L. Melamed et al.

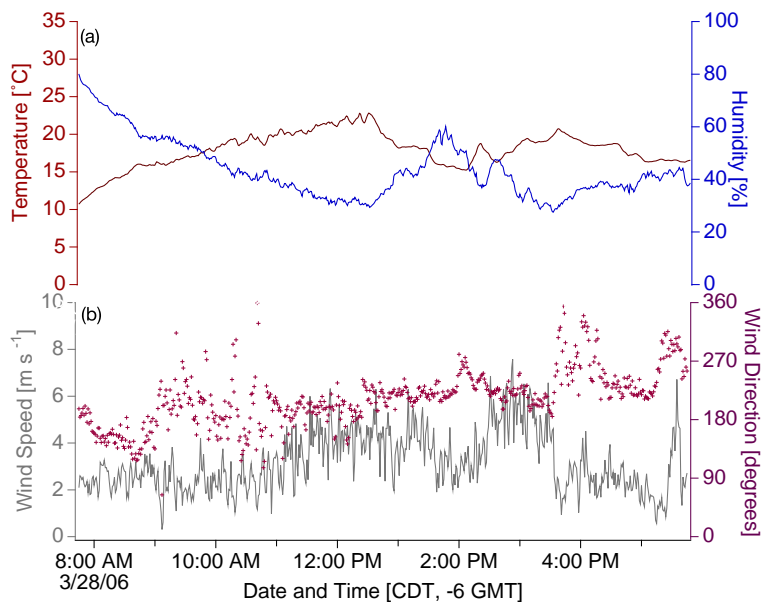


Fig. 11. Meteorological condition for 28 March 2006 at Tenango del Aire **(a)** air temperature and relative humidity and **(b)** wind speed and wind direction.

[Title Page](#)[Abstract](#)[Introduction](#)[Conclusions](#)[References](#)[Tables](#)[Figures](#)[◀](#)[▶](#)[◀](#)[▶](#)[Back](#)[Close](#)[Full Screen / Esc](#)[Printer-friendly Version](#)[Interactive Discussion](#)

**NO₂ DOAS
measurements at
Tenango del Aire**

M. L. Melamed et al.

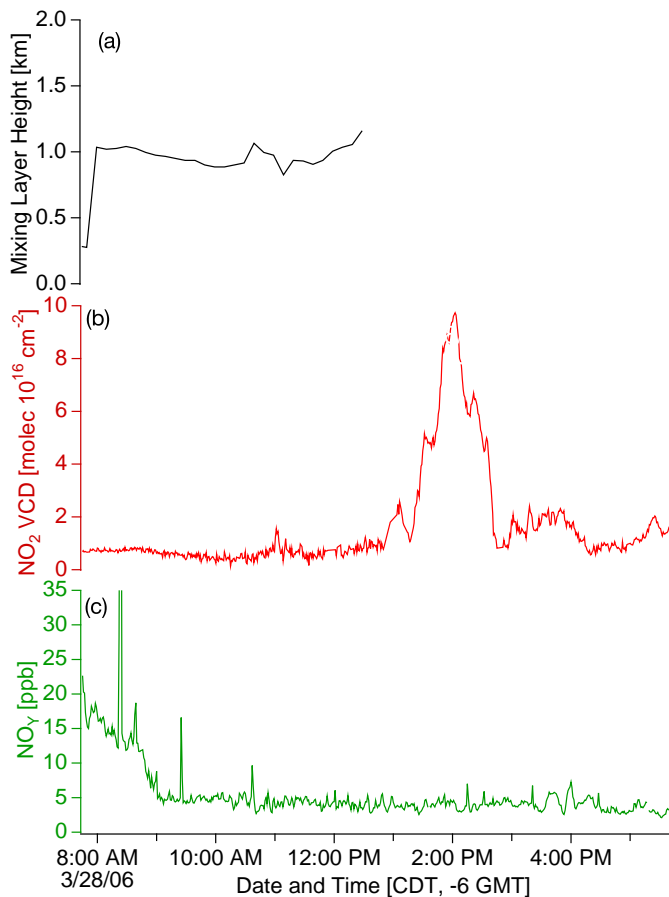


Fig. 12. Measurements of **(a)** ceilometer mixing layer height **(b)** DOAS NO₂ vertical column densities and **(c)** surface NO₂ on 28 March 2006.

[Title Page](#)[Abstract](#)[Introduction](#)[Conclusions](#)[References](#)[Tables](#)[Figures](#)[◀](#)[▶](#)[◀](#)[▶](#)[Back](#)[Close](#)[Full Screen / Esc](#)[Printer-friendly Version](#)[Interactive Discussion](#)

**NO₂ DOAS
measurements at
Tenango del Aire**

M. L. Melamed et al.

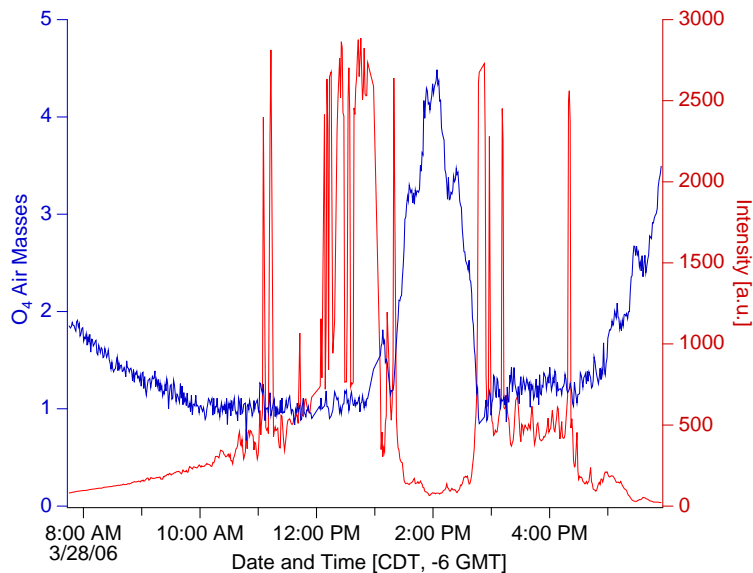


Fig. 13. The O₄ AMF (blue line) and intensity (red line) of photons reaching the spectrometer in the wavelength region of the O₄ retrievals on 28 March 2006.

[Title Page](#)[Abstract](#)[Introduction](#)[Conclusions](#)[References](#)[Tables](#)[Figures](#)[◀](#)[▶](#)[◀](#)[▶](#)[Back](#)[Close](#)[Full Screen / Esc](#)[Printer-friendly Version](#)[Interactive Discussion](#)

**NO₂ DOAS
measurements at
Tenango del Aire**

M. L. Melamed et al.

Title Page

Abstract

Introduction

Conclusions

References

Tables

Figures

◀

▶

◀

▶

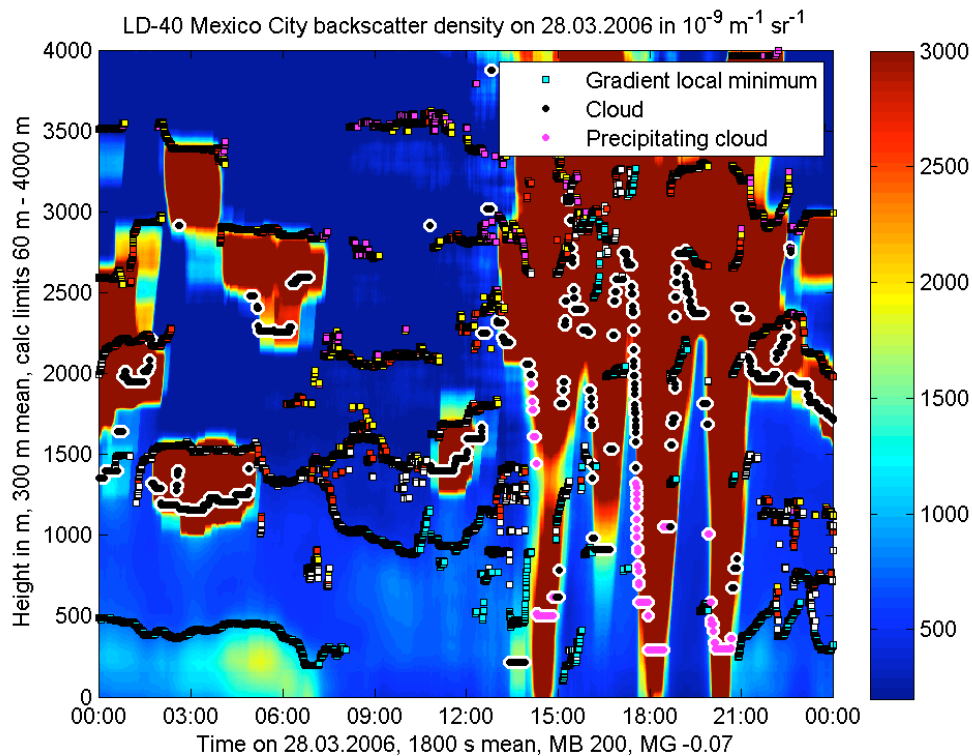
Back

Close

Full Screen / Esc

Printer-friendly Version

Interactive Discussion

**Fig. 14.** Ceilometer backscattering density on 28 March 2006.